Defining N-RAS signaling pathways essential for melanoma formation

Undergraduate Research Thesis

Presented in Partial Fulfillment of the Requirements for graduation *with Honors Research Distinction* in the undergraduate colleges of The Ohio State University

By

Aastha Dhakal

The Ohio State University

May 2019

Project Advisor: Dr. Christin E. Burd, Department of Molecular Genetics

Abstract

Targeted therapeutic options for the 15-25% of melanomas driven by oncogenic *N-RAS* mutations are currently unavailable. Therefore, immune-based therapies are the front-line treatment for these tumors. Unfortunately, only 40% of patients respond to immune-based therapies and numerous responders exhibit severe adverse events. Thus, it is important to find new therapeutic options for *N-RAS*-mutant melanomas. To understand the mechanism by which mutant N-RAS promotes melanoma formation, our laboratory developed a suite of genetically engineered mouse models (GEMMs) that enable conditional, melanocyte-specific knock-in of *N-Ras* mutations into endogenous alleles. We developed a total of five GEMMS containing *N-Ras* codon 61 mutations found commonly (Q61R, Q61K, Q61L) or uncommonly (Q61H, Q61P) in melanoma. Recent data from the laboratory show that GEMMs expressing melanoma-common N-Ras mutants exhibit reduced tumor latency and increased tumor burden as compared to those expressing *N-Ras* mutations privy to other tumor types.

I hypothesized that the melanoma-common *N-RAS* mutations differentially utilize the canonical N-RAS signaling pathway (PI3K-AKT, RAF-MEK-ERK) to alter cellular proliferation and more effectively drive melanoma formation. Analyses of cell proliferation in mouse embryonic fibroblasts (MEFs) demonstrated that all of the aforementioned mutations increased proliferation levels similarly as compared to wild-type (WT) MEFs. However, immunoblots examining downstream pathways revealed no differences in the levels of phosphorylated ERK and AKT. Thus, analyzing these pathways in melanocytes within the skin of our GEMMs could illustrate the differences between the potent and non-potent melanoma-driving *N-RAS* mutations as tumor microenvironment could affect the signaling pathways. Additionally, testing of WT RAS activity revealed that there is a difference in levels of GTP-bound WT H-/K-Ras within our MEFs expressing various *N-Ras*^{Q61} mutations. Further elucidation of the signaling pathways and functions that enable a subset of *N-RAS* mutations to more effectively drive melanoma formation will allow us to identify novel therapeutic targets for this disease.

Introduction

Melanoma

The incidence of cutaneous melanoma is continuing to rise in many parts of the United States with over 96,480 new cases and over 7,230 estimated deaths expected in 2019 [1]. Based on the prevalence of mutated driver genes, melanoma can be classified into four subtypes: *B-RAF*-mutant, *N-RAS*-mutant, *NK1*-mutant, and triple wildtype [2]. Activating mutations in *N-RAS* and *B-RAF* are observed in 10-25% and 35-50% of all cutaneous melanomas, respectively [2]. There are successful targeted therapies available for B-RAF-mutant melanoma [3], but there are no effective targeted therapies for N-RAS-mutant melanoma [4]. Although the 2-5-year survival rate of melanoma patients treated with immune-based therapy is around 40%, many individuals do not receive long-term benefit, and a significant number experience severe, adverse events [4-6]. N-RAS does not have a suitable drug-binding pocket, thus, designing treatments that directly target N-RAS has proven difficult [7]. As there are no targeted therapies for N-RAS-mutant melanoma, it is necessary to explore functions of *N-RAS* mutations found in melanoma to find suitable targets for novel therapies.

The Ras Signaling Pathway

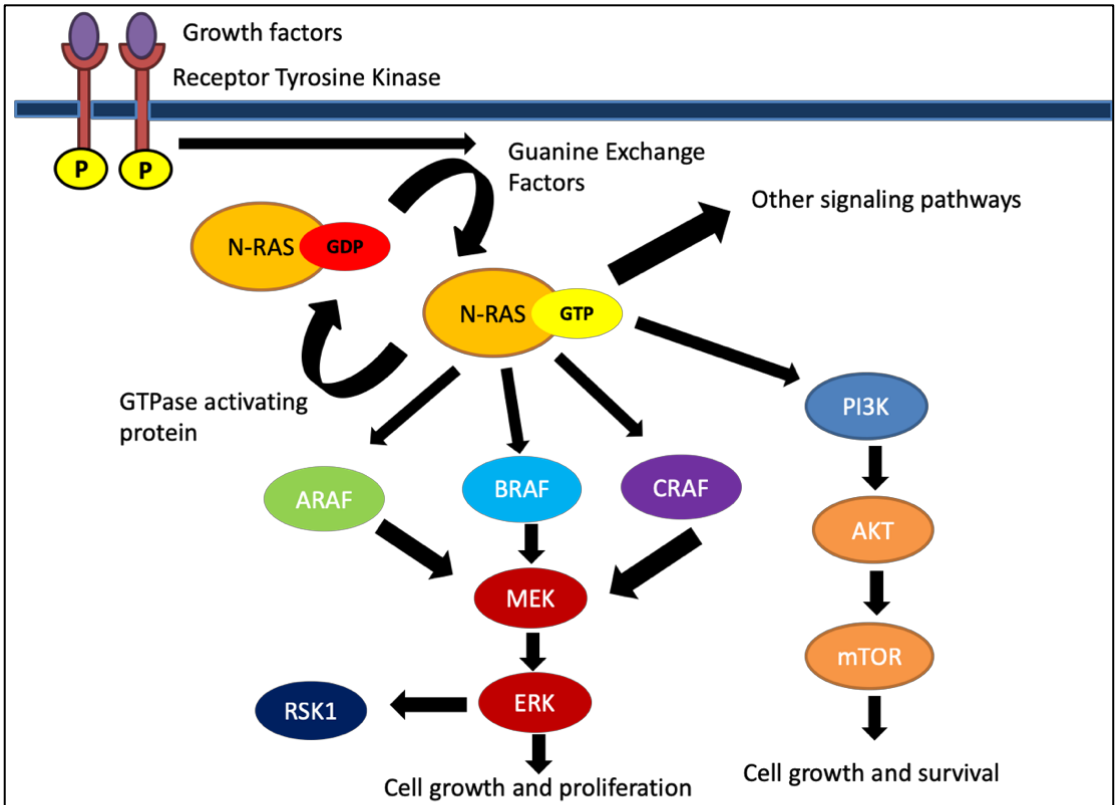

Figure 1: Canonical N-RAS signaling pathway. Adapted from Cox et al 2010 (Figure 2 and Figure 11). After N-RAS is activated through GTP binding, NRAS activates RAF-MEK-ERK and PI3K-AKT pathways to promote cell growth and proliferation.

N-RAS is a type of RAS protein, a GTPase essential for cell differentiation, survival, and proliferation [8]. There are four types of RAS proteins encoded by separate genes: H-RAS, K-RAS4A, K-RAS4B, and N-RAS [9]. Activation of RAS depends on receptor tyrosinase kinase (RTK) activity. The binding of growth factors to RTK activates Guanine Nucleotide Exchange Factors (GEFs, **Figure 1**). These activated GEFs facilitate the release of GDP and binding of GTP to RAS, resulting in an activated RAS that initiates several signaling cascades (RAF-MEK-ERK, PI3K-AKT) (**Figure 1**). GTPase activating proteins (GAPs) catalyze hydrolysis of GTP to GDP of RAS-bound GTP [10] (**Figure 1**) reverting the protein to an inactivated state.

Mutations affecting N-RAS codons 12 and 13 limit GAP binding to N-RAS [11], while mutations affecting N-RAS codon 61 cause a change in the catalytic site—disabling GTP hydrolysis [12]. In

both cases, N-RAS becomes constitutively active, leading to uncontrollable cell division and growth.

Mutation Specificity in N-RAS-Mutant Cancers

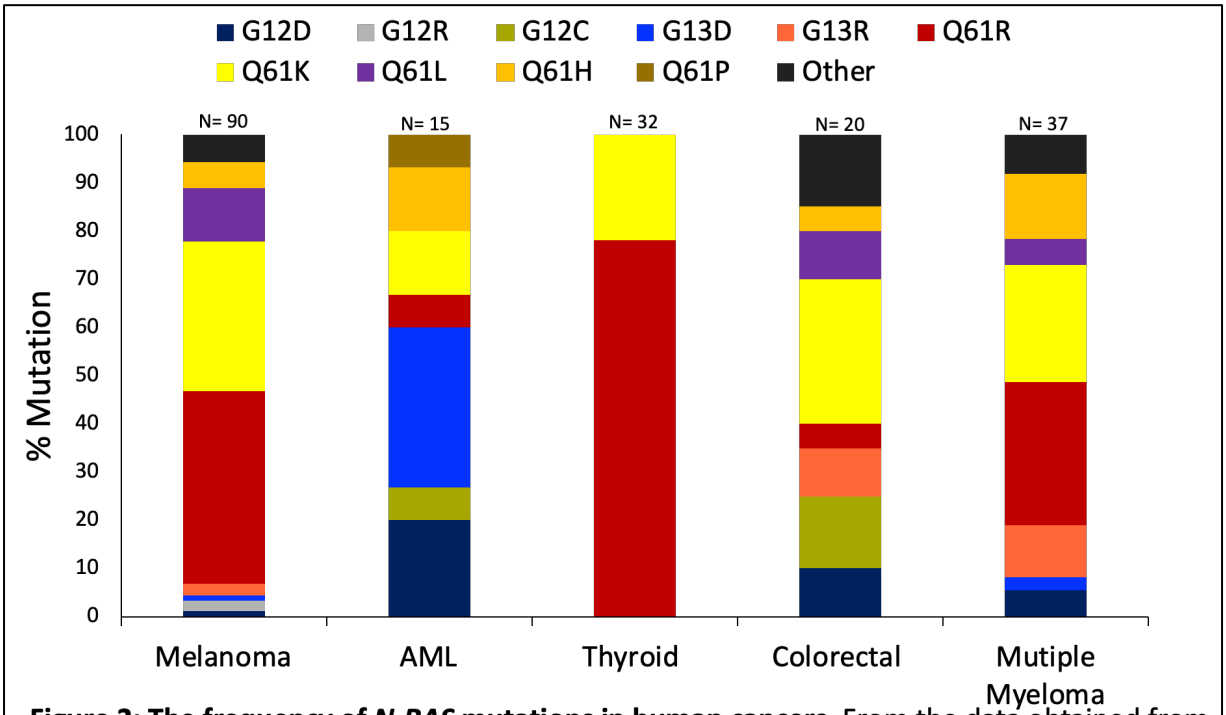

Figure 2: The frequency of *N-RAS* mutations in human cancers. From the data obtained from cBioPortal for Cancer Genomics, the graph shows the percentage of specific *N-RAS* mutations prevalent in cancers associated with an oncogenic *N-RAS* mutation.

N-RAS mutations in human melanoma are commonly localized to codon 61 with the most frequent mutations being Q61R, Q61K, or Q61L [13-15] (**Figure 2**). Additional *N-RAS* mutations are found in other cancer types, for example G12D/C, G13D, and Q61P/H are commonly observed in acute myeloid leukemia [13, 14] (AML; **Figure 2**). Mutations in codons 12, 13 or 61 lead to activated N-RAS, however, the mutant N-RAS could have different functions depending on the cell type. The prevalence of specific *N-RAS* mutations in each form of cancer could be due to the selection of a mutational event that is required for the transformation of tissue-specific cell type (i.e melanocytes in melanoma, leukocytes in leukemia etc.). The mutation in codon 61 could drive functions that are required to transform melanocytes but not white blood cells, leading to

melanoma, but not AML. Exploring the functions of different *N-RAS* mutations will redefine research and clinical approaches to N-RAS-driven cancers.

Hypotheses Regarding Oncogenic *N-RAS* mutations

To explain the prevalence of specific *N-RAS* mutations in cancer, there are two favored hypotheses. Activated and oncogenic N-RAS proteins signal through multiple downstream pathways to stimulate cellular proliferation and survival, leading to increased cell division and decreased cell death [16]. The first hypothesis is that the over-activation of N-RAS downstream pathways are drivers for melanoma development. The second hypothesis focuses on the effect of mutant RAS protein on the wildtype (WT) cognate and non-cognate isoforms. Cognate isoform refers to the same isoform as the mutant (i.e. WT K-Ras is cognate to K-Ras^{mut}) while non-cognate isoforms refer to a different isoform than the mutant (i.e. H-Ras is non-cognate K-Ras^{mut}). Investigations on the role of WT RAS in the presence of mutated RAS has revealed that non-cognate WT RAS has tumor-promoting activity while cognate WT RAS has tumor-suppressing activity [17-19]. Therefore, it is hypothesized that activation of WT H-/K-RAS contribute to proliferation of cells in N-RAS-mutant melanoma. However, there is little understanding of the specific roles of the two WT isoforms in N-RAS-driven cancers [17].

As both the hypotheses consider different interactions of N-RAS to explain the prevalence of *N-RAS* mutations in cancers, the hypotheses are not mutually exclusive. The activation of downstream pathways of N-RAS as well as the activity of WT H-/K-RAS could contribute to the tumorigenic potential of *N-RAS* mutations.

Study Rationale

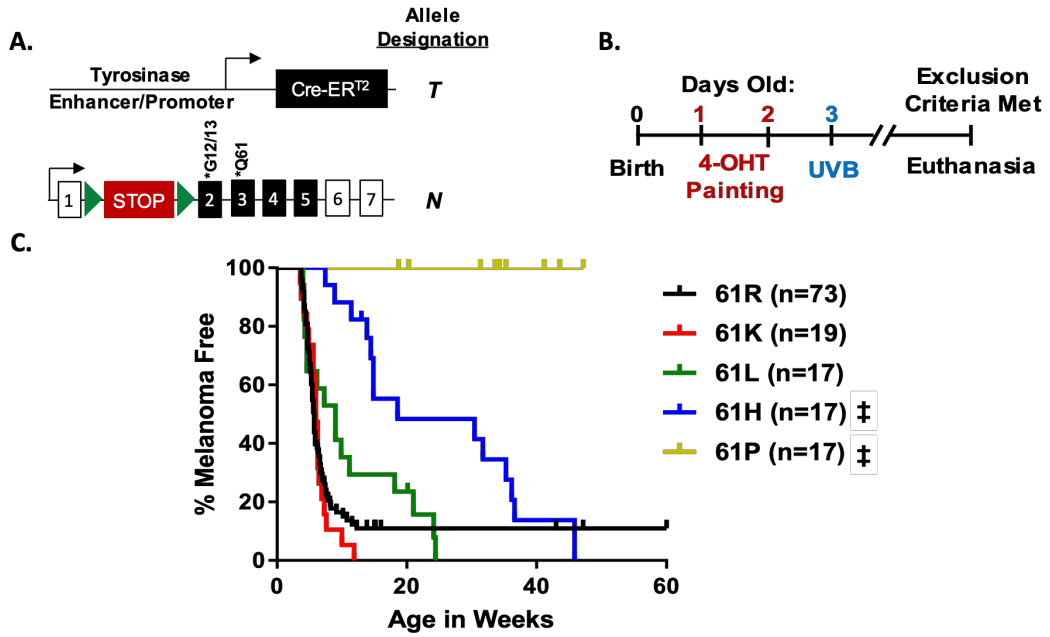

Figure 3. *LSL-NRas* melanoma models. A) Diagram of genetically engineered murine alleles and designations. *T* – transgenic *Cre-ER*^{T2} (Cre-ER^{T2} : Cre-tagged Estrogen Receptor specific to tamoxifen) allele driven by a melanocyte-specific *tyrosinase* enhancer; *N* – modified endogenous *NRas* allele; Green triangles – LoxP/Cre-recognition sites; STOP – transcriptional stop sequence. **B)** Schematic representation of the experimental protocol. Topical application of 20 mM 4-hydroxytamoxifen (4-OHT) is used to induce Cre-ER^{T2} activity in melanocytes. UV is administered as a single 4.5 kJ/m^2 dose using a fixed position, 16W, 312nm UVB light source. **C)** *In-vivo* data (Murphy et al. in preparation) showing melanoma-free survival of *TN* mice homozygously expressing various *NRas* codon 61 mutations. Statistical significance is designated as follows: ‡ p< 0.001.

By understanding the functional differences between melanoma-common and uncommon *N-RAS* mutations, we can identify potential therapeutic targets to treat N-RAS-driven melanoma. To study N-RAS-mutant melanoma, our laboratory developed genetically engineered murine models (GEMMS) with conditional knock-in melanoma-common and -uncommon *N-RAS* mutations (**Figure 3A**). Through these GEMMS, we have found that Q61R/K/L GEMMs have an earlier onset of melanoma compared to Q61H/P (Hennessey et al. in preparation, Murphy et al. in preparation, **Figure 3C**). Based upon these observations, **I hypothesized that the melanoma-**

common N-RAS mutations differentially utilize the canonical N-RAS signaling pathway (PI3K-AKT, RAF-MEK-ERK) to alter cellular proliferation and more effectively drive melanoma formation. To test this hypothesis, I used Murine Embryonic Fibroblasts (MEFs) extracted from each of our GEMMs to analyze the proliferative behavior of cells carrying the aforementioned *N-Ras* alleles and the effect of these alleles on downstream signaling. I also examined the activity of WT H-/K-Ras isoforms in the presence of N-Ras-mutants. By examining the effects of melanoma common and-uncommon *N-Ras* mutations, we can gather information that will help us understand why certain *N-Ras* mutations drive melanoma formation to later develop effective therapies.

Materials & Methods

Mouse protocol

The mouse handling protocols and procedures were reviewed and approved by The Ohio State University's Institutional Animal Care and Use Committee (Protocol #2012A00000134).

N-Ras Induction in MEFs

Mouse embryonic fibroblasts (MEFs) were isolated from our N-Ras mutant GEMMs on embryonic day 13.5. One million second passage MEFs were infected with Adenoviral Cre recombinase or GFP control at a multiplicity of infection of 4000:1. Cells were infected for 18 h in 0.5% DMEM. After infection, cells were grown in 10% DMEM.

Proliferation analysis

Three and seven days following adenoviral infection, MEFs were placed in serum starved conditions (0.5% serum) for 4 hours and labeled for 4 hours with 10 μM of 5-ethynyl-2′-deoxyuridine (EdU). MEFs were harvested and processed using the Click-iT EdU Flow Cytometry

Assay Kit as described by the manufacturer (Invitrogen, C10634). Briefly, the MEFs were fixed in cold 4% paraformaldehyde and then permeabilized with 1X Invitrogen saponin buffer. The cells were then labeled with 642 fluorescent azide (Active Motif #15288) and analyzed on BD Biosciences LSRII flow cytometer. The resulting data were visualized and quantified using FlowJo® software. Data of each sample was compared to WT using one-way ANOVA with Dunnett's test correcting for multiple comparison.

Immunoblotting

Three and seven days after adenoviral infection, MEFs were incubated for 16 hours in 0.5% DMEM and then the cells were harvested and lysed in RIPA (50 mM Tris pH 8.0, 150 mM NaCl, 1% IGEPAL-CA -630, 0.5% deoxycholate, 0.1% (w/v) SDS) containing protease inhibitor (Sigma, P8340). Proteins were separated by SDS-PAGE (12%, w/v) and transferred to a 0.2 μm PVDF membrane (100 V, 50 min). The membrane was blocked in 5% (w/v) milk for 30 min and incubated with primary antibodies generated against the following targets: phosphorylated ERK (Cell Signaling, 9101), total ERK (Cell Signaling, 4696) phosphorylated AKT (Cell Signaling, 9271S), total AKT (Cell Signaling, 2920S), or N-RAS (Abcam, ab77392), overnight. Fluorescently-tagged secondary antibodies (LI-COR IRDye 680, 800) were used to visualize each protein. The membranes were imaged on an LI-COR Odyssey® CLx and quantified using Image Studio® software. Data of each sample was compared to WT using one-way ANOVA with Dunnett's test correcting for multiple comparison.

GST-pull down assays

Isopropyl β-D-1-thiogalactopyranoside (IPTG) (0.3 mM) was added to bacteria containing an inducible GST-tagged RAF1-RBD plasmid and grown for 3 hours. The resulting cells pellets were lysed in bacterial lysis buffer (20mM Tris-HCl pH 8.0, 100mM NaCl, 1mM EDTA pH 8.0, 0.5% Sarkosyl). Glutathione (GSH) embedded agarose beads (Thermo Scientific, 16100) were

incubated with bacterial cell lysate containing recombinant GST-tagged RAF1-RBD for 45 min. Adenoviral Cre infected MEFs were grown to 70-80% confluency and lysed in NETN buffer (20mM Tris-HCl pH 8.0, 100 mM NaCl, 1mM EDTA pH 8.0, 0.5% NP-40). One hundred μg of input was saved from the whole lysate sample. Active GTP-bound Ras was isolated from 5.5 mg of whole cell lysate by incubating with 35 μL GSH agarose beads conjugated to GST-RAF1-RBD. Protein bound to the RAF1-RBD beads was analyzed by immunoblotting using primary antibodies directed against the following proteins: H-RAS (Abcam, ab32417) and Pan-Ras (Millipore Sigma, OP40-100UG). Fluorescently-tagged secondary antibodies (LI-COR IRDye 680, 800) were used to visualize bound primary antibody. The membranes were imaged on Odyssey® CLx.

Results

N-Ras-mutant MEFs exhibit similar proliferative behavior

Our *in vivo* data showed that mice expressing melanoma common *N-Ras* mutations (Q61R/K/L) have faster tumor onset (**Figure 3**), compared to those expressing melanoma-uncommon *N-Ras* mutations (Q61H/P). One element that drives cancer initiation is aberrant proliferation. Therefore, we postulated that primary untransformed cells expressing melanoma-common *N-Ras* mutations have increased proliferation compared to cells expressing melanoma-uncommon *N-Ras* mutations. To determine if N-Ras-mutants have distinct abilities to drive proliferation we examined the rate of EdU incorporation in MEFs from each our models. Supplementation of EdU, a thymidine analogue, in the growth media leads to labeling of DNA in replicating cells. Cells were infected overnight with adenoviral controls or Cre recombinase, and then allowed to recover in fresh media. Three and seven days after adenoviral infection, cells were placed in serum-starved condition for 4 h before cells were grown in EdU for additional 4 h. EdU-labeled MEFs were fixed and the percentage of EdU positive cells were determined by flow cytometry. At three and seven days, N-Ras-null and WT MEFs had similar levels of EdU positive cells (~23% and ~20% at 3

days; ~16% and ~15% at 7 days, respectively; **Figure 3B & C**). By contrast, all MEFs expressing oncogenic *N-Ras* showed increased levels of EdU positive cells when compared to control cells at 3 and 7 days post-Cre (~22-30% at 3 days post-Cre; ~22-28% at 7 days post-Cre; **Figure 3B & C).** Therefore**,** although N-Ras-mutant MEFs exhibit higher proliferation rates when compared to N-Ras-null and WT MEFs, these data showed that all of the *N-Ras* mutations drive proliferation equally.

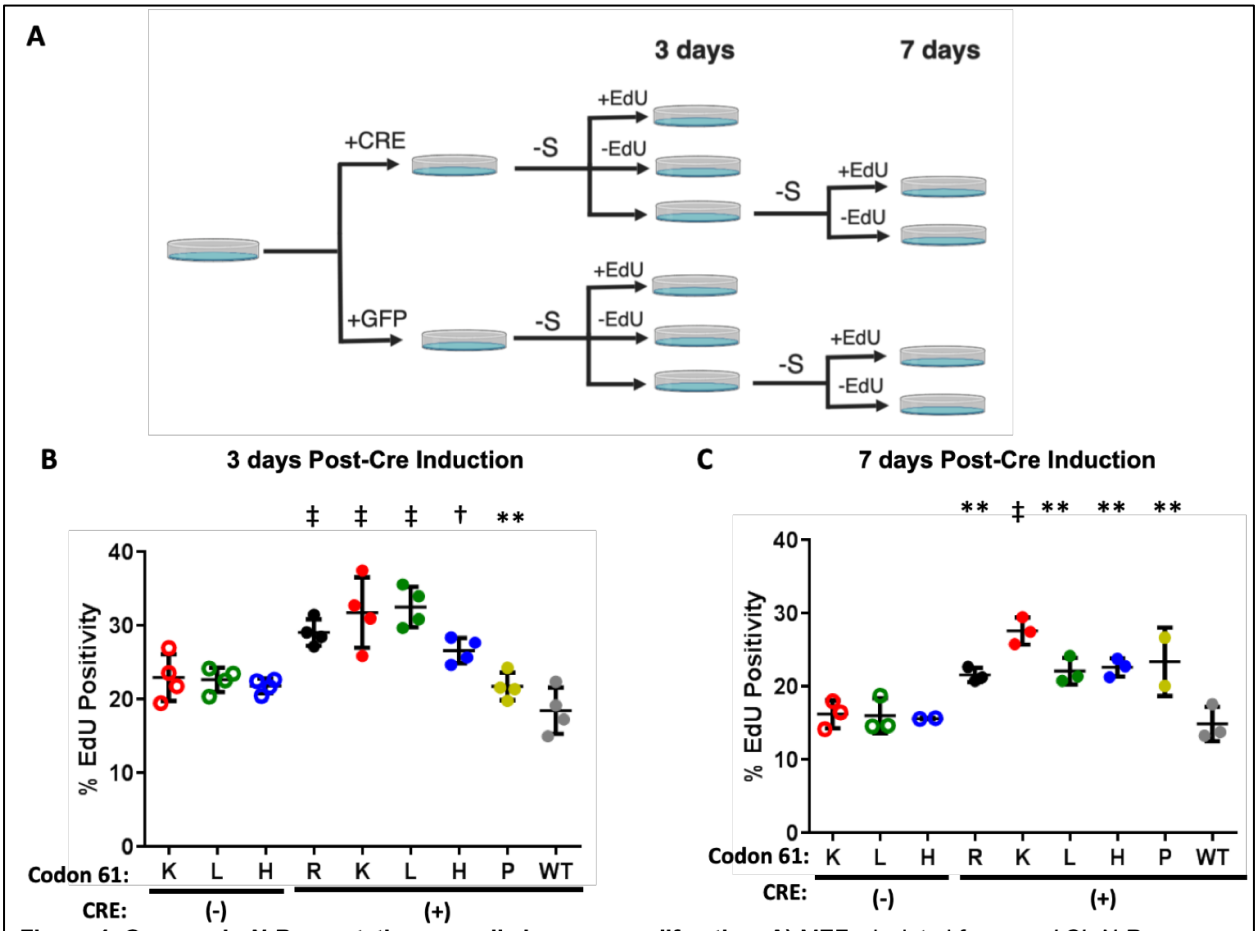

Figure 4: Oncogenic *N-Ras* mutations equally increase proliferation. A) MEFs, isolated from our *LSL-N-Ras* mouse model, were grown overnight in serum starved conditions (0.5% serum DMEM, -S) with adenoviral Cre recombinase or GFP control. Three and seven days after the addition of adenovirus, cell were to incubated for 4 h in 0.5% serum DMEM (-S) then labeled for 4 h with EdU in 0.5% serum DMEM. **B & C)** Scatter plots showing the average percentage of EdU positive cells across four biological replicates with error bars representing the standard deviation. Results are shown for EdU assays conducted Three **(B)** and seven **(C)** days after the addition of adenovirus**.** Mean of each sample was compared to WT using one-way ANOVA with Dunnett's test to correct for multiple comparisons. Statistical significance is designated as follows ** $p < 0.01$, † $p < 0.001$, ‡ $p < 0.0001$.

Similar levels of phosphorylated ERK and AKT in N-Ras-mutant and WT MEFs

Similar to Ras isoforms interacting differently with downstream effectors [20, 21], we hypothesized that melanoma-common N-Ras-mutants could differentially affect downstream signaling pathways, resulting in early melanoma onset compared to melanoma-uncommon N-Ras-mutants. Therefore, we were interested in examining N-Ras canonical signaling pathways (RAF-MAPK-ERK, PI3K-AKT), specifically levels of phosphorylated ERK and AKT, in cells expressing various *N-Ras* mutations. MEFs were transfected overnight with adenoviral control or Cre recombinase and allowed to rest after a media change. Three and seven days after adenoviral infection, cells were placed in serum starved condition for 16 h and the levels of total and phosphorylated ERK and AKT were analyzed through immunoblotting. The signals for all the samples were normalized to WT sample. All N-Ras-mutant MEFs exhibited similar levels of phosphorylated ERK and AKT as that of N-Ras null and WT MEFs (**Figures 4 & 5**, respectively). These results indicate that there are no difference in activation of MAPK and PI3K pathways in melanoma-common and-uncommon *N-Ras* mutations.

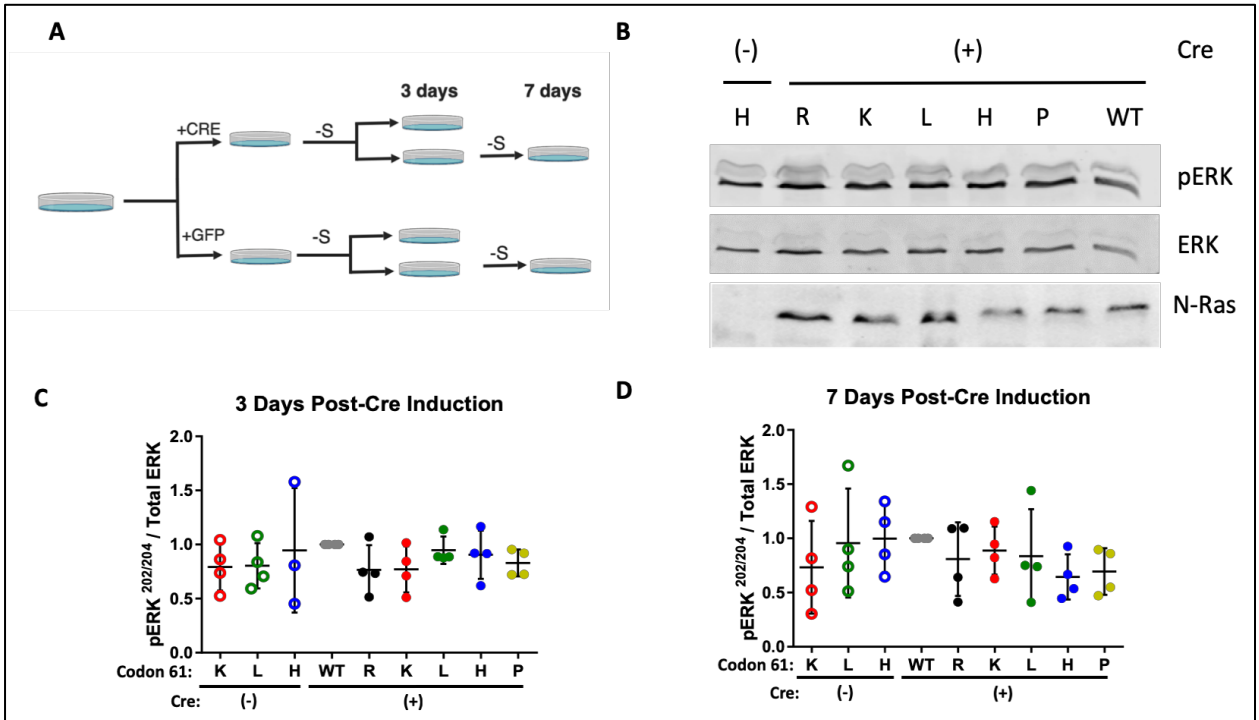

Figure 5: N-Ras-mutants drive similar levels of phosphorylated ERK. A) MEFs, isolated from our *LSL-N-Ras* mouse model, were grown overnight in serum starved conditions (0.5% serum DMEM, -S) with adenoviral Cre recombinase or GFP control. Three and seven days after the addition of adenovirus, the cells were harvested, lysed, and quantified. Cell lysates were analyzed by SDS-PAGE followed by immunoblotting with antibodies recognizing phosphorylated and total ERK. **B)** A representative image of an immunoblot showing phosphorylated ERK (Thr202/204), total ERK, and N-Ras. **C & D)** Scatterplots showing phosphorylated ERK levels normalized to total ERK. Four biological replicates with error bars representing the standard deviation are shown for samples three **(C)** and seven **(D)** days after N-Ras induction.

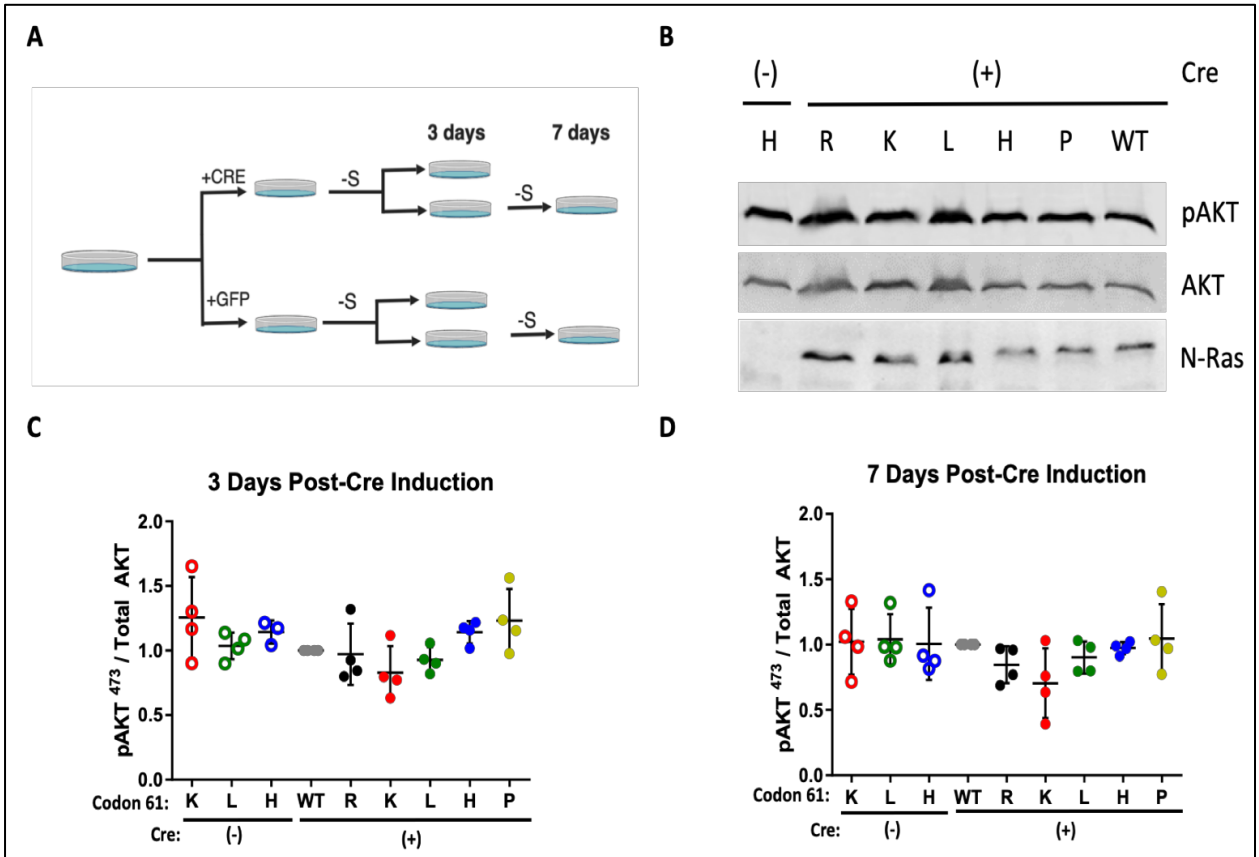

Figure 6: N-Ras-mutants drive similar levels of phosphorylated AKT. A) MEFs, isolated from our *LSL-N-Ras* mouse model, were grown overnight in serum starved conditions (0.5% serum DMEM, -S) with adenoviral Cre recombinase or GFP control. Three and seven days after the addition of adenovirus, the cells were harvested, lysed, and quantified. Cell lysates were analyzed by SDS-PAGE followed by immunoblotting with antibodies recognizing phosphorylated and total AKT. **B)** A representative image of an immunoblot showing phosphorylated AKT (Ser473), total AKT, and N-Ras. **C & D)** Scatterplots showing phosphorylated AKT levels normalized to total AKT. Four biological replicates with error bars representing the standard deviation are shown for samples three **(C)** and seven **(D)** days after N-Ras induction.

Difference in WT H-/K-Ras levels in MEFs with oncogenic *N-Ras* mutations

Mutant K-RAS leads to activation of WT H- and N-RAS, but the effect of mutant N-RAS on WT H- and K-RAS is not well understood [17]. Thus, we sought to examine the differences in activated WT H- and K-Ras in N-Ras-mutant cells. We performed activated Ras pull-down assays to determine whether there were differences in the levels of activated wildtype H-/K-Ras proteins in MEFs expressing *N-Ras*^{Q61R} or *N-Ras*^{Q61K} melanoma-common) and MEFs expressing *N-Ras*^{Q61H} (melanoma-uncommon). After inducing the production of GST-tagged RAF1-RBD in bacteria, the bacterial lysate was incubated with glutathione beads (**Figure 6A**) to immobilize the RAF1-RBD (Ras binding domain). The beads were then incubated with lysates from *N-Ras*^{Q61R}, *N-Ras*^{Q61K},

or *N-Ras*^{Q61H} expressing MEFs. To confirm the presence of H-, K-, and N-Ras in samples used for the pull-down assay, a portion of each lysate was saved. Activated wildtype H- and K-Ras bound to the RAF-RBD beads was detected using SDS-PAGE followed by immunoblotting. H-Ras-specific antibody was used to visualize WT H-Ras, while K-Ras was identified by using Pan-Ras antibody and observing bands of the appropriate molecular weight. The input confirmed the presence of H-/K-/N-Ras in MEF lysates (H-Ras, **Figure 7B**; H-/K-/N-Ras, **Figure 7C**). As N-Ras^{Q61H} interacts differently with the SDS-PAGE gel, it appears to be the same weight as H-Ras (**Figure 7C**). Activated H-Ras and K-Ras were found at higher levels in the Q61K N-Ras-mutant when compared to the Q61R and Q61H N-Ras-mutants. However, more biological replicates of this experiment are needed to support this conclusion.

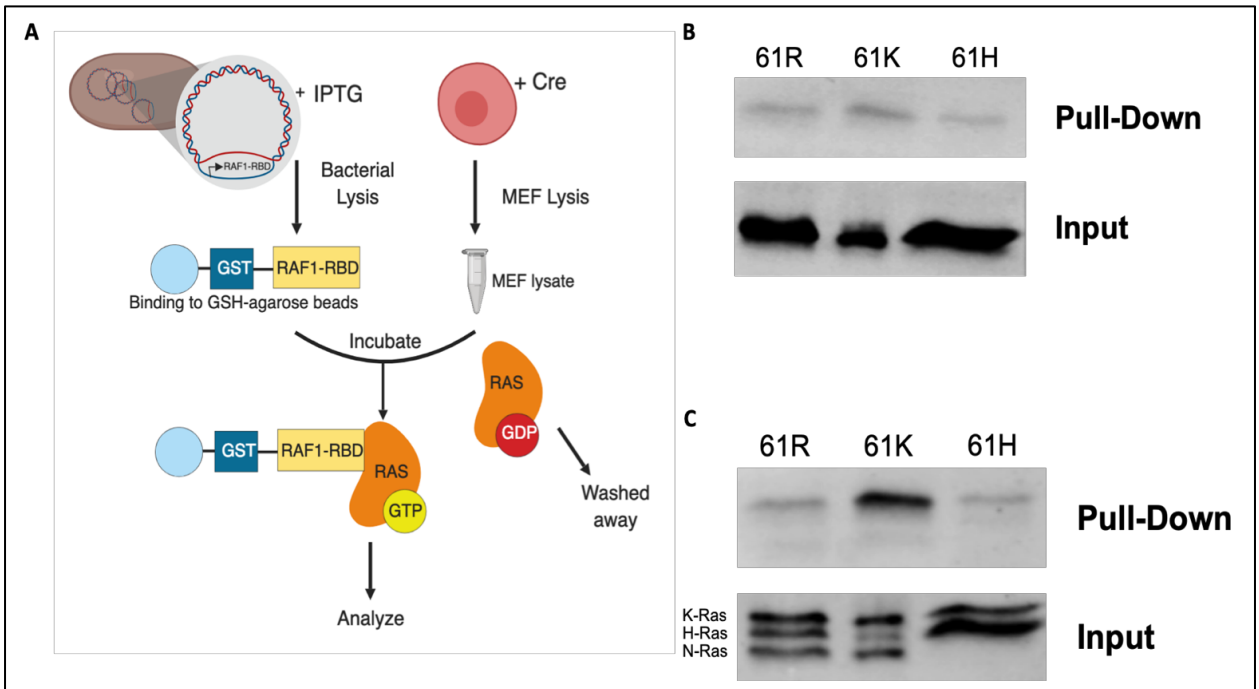

Figure 7: Levels of activated WT Ras in MEFs with *N-Ras* mutations. A) Bacteria with inducible GST-tagged RAF1-RBD was induced with IPTG for 3 h to initiate expression of this recombinant protein. The bacterial lysate was incubated with GSH agarose beads to generate beads bound with GST-RAF1-RBD. MEFs with induced N-Ras expression (+ Cre) were lysed and incubated with the GST-RAF1-RBD beads. Activated GTP-bound Ras interacting with RAF1-RBD was isolated and analyzed by SDS-PAGE followed by immunoblotting with antibodies recognizing H-Ras and Pan-Ras. **B)** An immunoblot image showing H-Ras signal in the input and pull-down assays using Q61R, Q61K, and Q61H MEFs. **C)** An immunoblot image that shows K-Ras signal (identified by the size) after probing for Pan-Ras in the input and pull-down assays using Q61R, Q61K, and Q61H MEFs.

Discussion

This study reveals the proliferative behavior, signaling, and potential role of WT H-/K-Ras in N-Ras-driven cancers. We find that N-Ras-mutant cells exhibit similar rates of proliferation and levels of phosphorylated ERK and AKT, yet WT H-/K-Ras are more active in the presence of melanoma-common N-Ras mutants. In this study, we addressed the question of why certain *N-Ras* mutations lead to melanoma, and our findings promote the foundation for future experiments that could help us understand the mechanisms necessary for melanoma formation.

Proliferation of N-Ras mutant MEFs

We observed that all *N-Ras* mutations promote proliferation equally, thus not supporting our expectation that melanoma-common *N-Ras* mutations would show increased proliferation when compared to melanoma-uncommon *N-Ras* mutations. Previous research comparing colon cancer cells expressing *K-Ras*^{G12D} and *N-Ras*^{G12D} showed that cells with K-Ras mutants had increased proliferation [22], thereby demonstrating isoform-specific Ras activity. Similar to this distinct activity of mutant K-Ras and N-Ras in the colon, we expected that specific *N-Ras* mutations might differentially drive cellular proliferation, leading to melanoma formation. There is evidence to suggest that N-Ras-mutant melanoma is mutation-specific. Mice expressing *N-Ras*^{Q61R} develop melanoma, whereas those expressing *N-Ras*^{G12D} do not [23]. Our unpublished suite of *in vivo* mouse models also supports the hypothesis that melanomagenesis is mutation-specific. Melanoma onset is faster in mice expressing melanoma-common *N-Ras* mutations (Q61R/K/L) than in mice harboring melanoma-uncommon *N-Ras* mutations (Q61P/Q) (**Figure 3**). Thus, we expected melanoma-common N-Ras mutant MEFs to show increased proliferation. However, all of the *N-Ras* mutations in this study lead to constitutively active N-Ras, so observing equal rates of proliferation is not surprising. Juxtaposing the proliferation data with *in vivo* observations suggests that proliferation is not sufficient for transformation of cells. Proliferation also leads to

senescence, which is an irreversible cell cycle arrest. Therefore, there could be other mutant-specific N-Ras activities that lead to melanoma formation. Experiments investigating the rate of proliferation in melanocytes with various *N-Ras* mutations could provide insight into the functional differences between melanoma-common and -uncommon *N-Ras* mutations.

ERK and AKT signaling in N-Ras mutant MEFs

When examining signaling pathways downstream of Ras, our data revealed that there is no difference in the levels of phosphorylated ERK and AKT in N-Ras-null MEFs and MEFs expressing melanoma-common or -uncommon mutants. As studies have shown distinct signaling patterns downstream of H-, K-, and N-Ras isoforms [9], we hypothesized that there could be differential signaling in cells expressing melanoma-common and -uncommon N-Ras mutants. For example, one study showed that K-Ras4B^{G12V} engages Raf1 more effectively than K-Ras4A^{G12V}, N-Ras^{G12V}, and H-Ras^{G12V} [20]. Another study showed that H-Ras^{G12V} is a more potent activator of PI3K signaling than K-Ras^{G12V} in COS cells [21]. Based on these data, we expected that similar differences in signaling would be observed between melanoma-common and -uncommon N-Ras mutants, allowing us to understand the mechanism behind melanoma formation. The data showed that even N-Ras-null samples showed similar signaling when compared to the N-Ras-mutant MEFs, thus the data could be interpreted as the under-activation of RAF-MEK-ERK and PI3K-AKT pathway in N-Ras mutant cells. However, as the experiment was conducted in a static experimental condition, the N-Ras-null cells could have activated compensatory mechanisms that allow the cells to maintain basal level of phosphorylated ERK and AKT. Another reason for similar ERK and AKT signaling in N-Ras mutant MEFs compared to WT and N-Ras-null MEFs could be that melanoma-driving N-Ras mutants are more prone to interact with non-canonical downstream effectors, rather than ERK or PI3K. Proteomic analysis of melanoma-common and -uncommon N-Ras mutant MEFs could reveal differences in the cellular pathways activated by melanoma-common and -uncommon *N-Ras* mutations. Here, we used MEFs to examine downstream

signaling, so ERK and AKT signaling could be different when analyzing downstream signaling in melanocytes. We should also consider the tumor microenvironment and its effect in signaling. Thus, immunohistochemistry experiments that are designed to examine signaling in melanocytes and tumor cross-sections should be performed to understand the differences between melanoma-common and -uncommon *N-Ras* mutations.

Activated WT Ras isoforms in N-Ras mutant MEFs

The activated Ras pull-down assay revealed that there was a difference in wildtype H- and K-Ras activity in N-Ras Q61R, Q61K, and Q61H MEFs. As we observed higher levels of activated H- and K-Ras in the presence of N-Ras Q61K when compared to N-Ras Q61R/H, our data suggest that WT Ras could have different functions depending on the specific *N-Ras* mutation. Activated WT H- or K-Ras could be involved in driving the phenotype of earlier melanoma onset in GEMMs with melanoma-common *N-Ras* mutations. Published experiments involving knock-down of WT H- or N-Ras via shRNA in cancer cells with K-Ras^{G12D} or K-Ras^{G12C} mutants have shown that K-Ras mutant cells grow more slowly when the WT non-cognate Ras isoforms are not present [19, 24]. Results from this experiment suggested that WT H- or N-Ras are necessary to drive cell growth in K-Ras mutant cells, therefore, we postulated that WT non-cognate Ras isoforms could also play a tumor-promoting role in N-Ras mutant cells. Although more biological replicates are needed to draw a conclusion, we observed cells with N-Ras^{Q61K}mutant had higher levels of activated H-/K-Ras. Although N-Ras^{Q61K}mutant and N-Ras^{Q61R}mutant are both melanoma-common mutations, N-Ras^{Q61K}mutant exhibits higher levels of activated H-/K-Ras than N-Ras^{Q61R}mutant, suggesting that melanoma-common *N-Ras* mutations could have different mechanisms that lead to melanoma formation. For N-Ras^{Q61K}mutant, our data supports the hypothesis that WT non-cognate RAS isoforms have tumor-promoting functions in the context of tumor-promoting N-Ras mutants. Repeating the GST-pull-down assay with N-Ras-null MEF lysate could provide more information regarding levels of activated WT Ras in N-Ras mutant MEFs.

Performing enzyme-linked immune sorbent assay (ELISA) that examine levels of activated WT Ras would further validate the results. Experiments involving knock-down of WT H- and/or K-Ras in cells with melanoma-common and -uncommon *N-Ras* mutations will allow us to investigate the role of WT non-cognate Ras isoforms in N-Ras-driven melanoma.

In summary, this study has shown that there is no distinct proliferative behavior or canonical Ras signaling in MEFs expressing melanoma-common and -uncommon *N-Ras* mutations. However, melanoma-common N-Ras mutants could be utilizing non-canonical pathways, leading to N-Ras-driven melanoma. We observed an increase in activated WT H- and K-Ras levels in MEFs expressing $N\text{-}Ras^{Q61K}$ when compared to those expressing $N\text{-}Ras^{Q61R}$ and $N\text{-}Ras^{Q61H}$, and this finding could be a step towards understanding the mechanism for melanoma formation for the various N-Ras mutants. As targeting N-RAS directly has yet to be successful, it is necessary to explore functions unique to the melanoma-common *N-RAS* mutations to find alternative therapeutic approaches.

Acknowledgements

I would like to thank Dr. Christin Burd, Brandon Murphy, and other members of the Burd lab for helping me as well as Damon Runyun for funding the project. I would also like to thank the Pelatonia Undergraduate Fellowship for supporting this work.

References

1. Siegel, R.L., K.D. Miller, and A. Jemal, *Cancer statistics, 2019.* CA Cancer J Clin, 2019. **69**(1): p. 7-34.
2. Cancer Genome Atlas, N., *Genomic Classification of Cutaneous Melanoma.* Cell, 2015. **161**(7): p. 1681-96.
3. Kudchadkar, R., K.H. Paraiso, and K.S. Smalley, *Targeting mutant BRAF in melanoma: current status and future development of combination therapy strategies.* Cancer J, 2012. **18**(2): p. 124-31.
4. Johnson, D.B., et al., *Melanoma driver mutations and immune therapy.* Oncoimmunology, 2016. **5**(5): p. e1051299.
5. Prieto, P.A., et al., *CTLA-4 blockade with ipilimumab: long-term follow-up of 177 patients with metastatic melanoma.* Clin Cancer Res, 2012. **18**(7): p. 2039-47.
6. Johnson, D.B. and I. Puzanov, *Treatment of NRAS-mutant melanoma.* Curr Treat Options Oncol, 2015. **16**(4): p. 15.
7. Cox, A.D., et al., *Drugging the undruggable RAS: Mission possible?* Nat Rev Drug Discov, 2014. **13**(11): p. 828-51.
8. Malumbres, M. and M. Barbacid, *RAS oncogenes: the first 30 years.* Nat Rev Cancer, 2003. **3**(6): p. 459-65.
9. Castellano, E. and E. Santos, *Functional specificity of ras isoforms: so similar but so different.* Genes Cancer, 2011. **2**(3): p. 216-31.
10. Cox, A.D. and C.J. Der, *Ras history: The saga continues.* Small GTPases, 2010. **1**(1): p. 2-27.
11. Adari, H., et al., *Guanosine triphosphatase activating protein (GAP) interacts with the p21 ras effector binding domain.* Science, 1988. **240**(4851): p. 518-21.
12. Frech, M., et al., *Role of glutamine-61 in the hydrolysis of GTP by p21H-ras: an experimental and theoretical study.* Biochemistry, 1994. **33**(11): p. 3237-44.
13. Cerami, E., et al., *The cBio cancer genomics portal: an open platform for exploring multidimensional cancer genomics data.* Cancer Discov, 2012. **2**(5): p. 401-4.
14. Gao, J., et al., *Integrative analysis of complex cancer genomics and clinical profiles using the cBioPortal.* Sci Signal, 2013. **6**(269): p. pl1.
15. Carlino, M.S., et al., *Correlation of BRAF and NRAS mutation status with outcome, site of distant metastasis and response to chemotherapy in metastatic melanoma.* Br J Cancer, 2014. **111**(2): p. 292-9.
16. Vu, H.L. and A.E. Aplin, *Targeting mutant NRAS signaling pathways in melanoma.* Pharmacol Res, 2016. **107**: p. 111-116.
17. Zhou, B., C.J. Der, and A.D. Cox, *The role of wild type RAS isoforms in cancer.* Semin Cell Dev Biol, 2016. **58**: p. 60-9.
18. Young, A., D. Lou, and F. McCormick, *Oncogenic and wild-type Ras play divergent roles in the regulation of mitogen-activated protein kinase signaling.* Cancer Discov, 2013. **3**(1): p. 112-23.
19. Grabocka, E., et al., *Wild-type H- and N-Ras promote mutant K-Ras-driven tumorigenesis by modulating the DNA damage response.* Cancer Cell, 2014. **25**(2): p. 243-56.
20. Voice, J.K., et al., *Four human ras homologs differ in their abilities to activate Raf-1, induce transformation, and stimulate cell motility.* J Biol Chem, 1999. **274**(24): p. 17164-70.
21. Yan, J., et al., *Ras isoforms vary in their ability to activate Raf-1 and phosphoinositide 3-kinase.* J Biol Chem, 1998. **273**(37): p. 24052-6.
22. Haigis, K.M., et al., *Differential effects of oncogenic K-Ras and N-Ras on proliferation, differentiation and tumor progression in the colon.* Nat Genet, 2008. **40**(5): p. 600-8.

23. Burd, C.E., et al., *Mutation-specific RAS oncogenicity explains NRAS codon 61 selection in melanoma.* Cancer Discov, 2014. **4**(12): p. 1418-29.
24. Lim, K.H., et al., *Tumour maintenance is mediated by eNOS.* Nature, 2008. **452**(7187): p. 646-9.